Journal for
ImmunoTherapy of Cancer

Antitumor efficacy of ⁹⁰Y-NM600 targeted radionuclide therapy and PD-1 blockade is limited by regulatory T cells in murine prostate tumors

Hemanth K Potluri,[1] Carolina A Ferreira,[1,2] Joseph Grudzinski,[1,3] Christopher Massey,[1,3] Eduardo Aluicio-Sarduy,[2] Jonathan W Engle,[2,3] Ohyun Kwon [ORCID],[1,2] Ian R Marsh,[1,2,4] Bryan P Bednarz,[1,2] Reinier Hernandez,[1,2] Jamey P Weichert,[1,3] Douglas G McNeel [ORCID] [1]

[1]University of Wisconsin Carbone Cancer Center, University of Wisconsin-Madison, Madison, Wisconsin, USA
[2]Medical Physics, University of Wisconsin-Madison, Madison, Wisconsin, USA
[3]Radiology, University of Wisconsin-Madison, Madison, Wisconsin, USA
[4]Radiation Oncology and Molecular Radiation Sciences, Johns Hopkins University, Baltimore, Maryland, USA

Correspondence to
Dr Douglas G McNeel;
dm3@medicine.wisc.edu

ABSTRACT

Background Systemic radiation treatments that preferentially irradiate cancer cells over normal tissue, known as targeted radionuclide therapy (TRT), have shown significant potential for treating metastatic prostate cancer. Preclinical studies have demonstrated the ability of external beam radiation therapy (EBRT) to sensitize tumors to T cell checkpoint blockade. Combining TRT approaches with immunotherapy may be more feasible than combining with EBRT to treat widely metastatic disease, however the effects of TRT on the prostate tumor microenvironment alone and in combinfation with checkpoint blockade have not yet been studied.

Methods C57BL/6 mice-bearing TRAMP-C1 tumors and FVB/NJ mice-bearing Myc-CaP tumors were treated with a single intravenous administration of either low-dose or high-dose ⁹⁰Y-NM600 TRT, and with or without anti-PD-1 therapy. Groups of mice were followed for tumor growth while others were used for tissue collection and immunophenotyping of the tumors via flow cytometry.

Results ⁹⁰Y-NM600 TRT was safe at doses that elicited a moderate antitumor response. TRT had multiple effects on the tumor microenvironment including increasing CD8 +T cell infiltration, increasing checkpoint molecule expression on CD8 +T cells, and increasing PD-L1 expression on myeloid cells. However, PD-1 blockade with TRT treatment did not improve antitumor efficacy. Tregs remained functional up to 1 week following TRT, but CD8 +T cells were not, and the suppressive function of Tregs increased when anti-PD-1 was present in in vitro studies. The combination of anti-PD-1 and TRT was only effective in vivo when Tregs were depleted.

Conclusions Our data suggest that the combination of ⁹⁰Y-NM600 TRT and PD-1 blockade therapy is ineffective in these prostate cancer models due to the activating effect of anti-PD-1 on Tregs. This finding underscores the importance of thorough understanding of the effects of TRT and immunotherapy combinations on the tumor immune microenvironment prior to clinical investigation.

WHAT IS ALREADY KNOWN ON THIS TOPIC

⇒ External beam radiation therapy can sensitize tumors to checkpoint blockade. Targeted radionuclide therapy (TRT) is effective in treatment of prostate cancer.

WHAT THIS STUDY ADDS

⇒ This study describes the effects of TRT in the form of ⁹⁰Y-NM600 on the prostate tumor immune microenvironment and demonstrates that the combination of this TRT agent and PD-1 blockade is only effective when Tregs are depleted from the tumor.

HOW THIS STUDY MIGHT AFFECT RESEARCH, PRACTICE OR POLICY

⇒ The data presented here suggest that caution must be used when combining TRT and checkpoint blockade, a combination which is already the subject of multiple new clinical trials.

BACKGROUND

Radiation therapy has long been one of the mainstay treatments for prostate cancer.

External beam radiation therapy (EBRT) is a standard of care curative option for localized disease, but its role in widely metastatic disease has traditionally been limited to palliation of a small number of painful sites. An alternative method of treating pain from bone metastases at many sites was developed using systemic administration of radionuclides that are deposited in areas of active bone turnover, such as the beta-emitting radionuclides ^{89}Sr and ^{153}Sm.[1 2] This approach of using systemic radiation to treat all sites of metastatic disease simultaneously with relative sparing of healthy tissue is called targeted radionuclide therapy (TRT). Another bone-seeking agent, the alpha-emitting radionuclide ^{223}RaCl$_2$ (Xofigo), was US Food and Drug Administration (FDA)-approved for the treatment of metastatic castration-resistant prostate cancer (mCRPC) based on data showing extended

survival, though its efficacy is limited to patients with bony disease.[3]

More recently, there has been interest in developing TRTs that are targeted to prostate tumor cells rather than areas of bone remodeling, enabling them to be used for patients with visceral disease. One of the first TRT approaches used a radiolabeled antibody specific for prostate-specific membrane antigen (PSMA) called J591.[4 5] Subsequent efforts have focused on small molecules specific for PSMA such as [18F]DCFPyL and PSMA-617 which have both been used as positron emission tomography (PET) tracers.[6–13] PSMA-617 has also been radiolabeled with various radiometals including ^{90}Y, ^{177}Lu, and ^{225}Ac, and used therapeutically. Following the success of the VISION trial, ^{177}Lu-PSMA-617 has just received FDA approval for treatment of mCRPC.[14] While this TRT approach is a step forward in the treatment of mCRPC, it only extends survival by about 4 months.

Due to a large body of preclinical evidence suggesting that irradiating tumors can increase their susceptibility to immunotherapy, there is already much interest in combining ^{177}Lu-PSMA-617 and other TRTs with immunotherapy.[15–20] This may be particularly useful for prostate cancer for which immune checkpoint blockade monotherapy has yielded disappointing results.[21–23] Even low doses of radiation can induce an inflammatory response in poorly immunogenic tumors by increasing MHC-I expression on tumor cells, increasing cross-presentation by antigen-presenting cells, promoting Fas/Fas ligand (Fas-L) signaling, and inducing immunogenic cell death.[16 24 25] It has also been shown that the antitumor effects of radiation therapy are partly immune-mediated.[26] Two notable clinical trials have evaluated the combination of checkpoint blockade and EBRT in the metastatic setting. Both showed trends toward improvement in the combination arms but failed to reach prespecified endpoints.[27 28] It is possible that these trials were unsuccessful because radiation was delivered to only a small number of sites, leaving the other sites resistant to immunotherapy. TRT could therefore be an approach that overcomes this limitation. However, the effects of TRT on the prostate tumor immune microenvironment have yet to be characterized because most existing preclinical studies of TRT agents in prostate cancer have been performed in immunocompromised mice. Further, it is not known whether the combination of TRT and checkpoint blockade is effective in this disease.

Our group has used alkylphosphocholines (APCs), which have been shown to selectively accumulate in many tumor cell types via insertion into lipid rafts, as TRT agents.[29] First generation ^{131}I-NM404 is currently being investigated as a treatment for metastatic multiple myeloma and other cancers.[30–33] We have recently focused on evaluating the second generation APC, NM600, which can be radiolabeled with a variety of radiometals. By labeling with ^{86}Y, we can image tumors and perform dosimetry estimation via PET/CT, while by labeling with the isotopic pair, ^{90}Y, we are able to deliver therapeutic radiation. The relatively long 3.9 mm mean path length of ^{90}Y enables it to deliver homogenous radiation doses across a tumor, treating both cancer cells and surrounding cell types. This theranostic approach using ^{90}Y-NM600 has shown success in multiple preclinical models, but has not yet been evaluated in prostate cancer.[34–37]

In this report, we studied the effects of ^{90}Y-NM600 TRT on the prostate tumor immune microenvironment in two different strains of mice to evaluate its use in combination with immune checkpoint blockade. We found that ^{90}Y-NM600 increases CD8 +T cell infiltration while increasing PD-1 expression on CD8 +T cells. Unexpectedly, we observed that the combination of TRT and PD-1 blockade did not improve antitumor efficacy. We demonstrated that this lack of efficacy was mediated by the activating effects of PD-1 blockade on regulatory CD4 +T cells (Tregs) and that antitumor efficacy was improved by in vivo Treg depletion. These data underscore the importance of mechanistic understanding of the effects of TRT on the tumor microenvironment to best guide the timing and choice of combination therapies in prostate cancer.

METHODS

Radiosynthesis of $^{86/90}$Y-NM600

^{86}Y production, NM600 radiolabeling, and purification were performed as previously described.[34 36]

Cell lines

TRAMP-C1 (CRL-2730) and Myc-CaP (CRL-3255) cell lines were obtained from ATCC (Manassas, VA) and maintained according to ATCC recommendations. Cells were tested for mycoplasma contamination.

Mice

All animal studies were performed with approval from the University of Wisconsin Institutional Animal Care and Use Committee. C57BL/6J mice (stock #000664), FVB/NJ mice (stock #001800), and C57BL/6-Tg(Foxp3-DTR/EGFP)23.2Spar/Mmjax (DEREG, stock #32050-JAX) mice were obtained from The Jackson Laboratory (Bar Harbor, ME) and housed in microisolator cages under aseptic conditions.

Tumor implantation

Male C57/BL6 or DEREG mice aged 6–8 weeks were injected subcutaneously with 1×10^6 TRAMP-C1 cells in 50% Matrigel (Corning, Corning, NY CB354248) and 50% phosphate-buffered saline (PBS) in the right flank. Similarly, 1×10^6 Myc-CaP cells in PBS, without Matrigel, were implanted into the right flank of 6–8 weeks male FVB mice.

PET/CT imaging

PET/CT imaging was performed as previously described.[34 36] Briefly, mice-bearing TRAMP-C1 (n=4) or Myc-CaP tumors (n=3) were injected with 9.25 MBq of ^{86}Y-NM600 intravenously and sequential CT and static PET scans were acquired in an Inveon microPET/microCT

scanner (Siemens Medical Solutions, Knoxville, TN) at approximately 3, 24, 42, and 66 hours postradiotracer injection.

Dosimetry estimations

Dosimetry estimations were performed as previously reported using a Monte Carlo-based dosimetry assessment platform, Radionuclide Assessment Platform for Internal Dosimetry.[38–40]

Tumor growth studies

Tumors were measured twice weekly via calipers. Tumor volume was calculated as (long axis x short axis^2)/2. Mice were randomized to treatment groups and treatment was initiated once tumor volumes reached 100–200 mm^3.

^{90}Y-NM600 TRT

Either 50 µCi (1.85 MBq; low dose) or 250 µCi (9.25 MBq; high dose) of ^{90}Y-NM600 was injected into the tail vein of tumor-bearing mice. Based on dosimetry studies as described above, we estimate that low-dose TRT delivered 1–2 Gy to TRAMP-C1 tumors and 3–4 Gy to Myc-CaP tumors, while high-dose TRT delivered 5–6 Gy to TRAMP-C1 tumors and 16–20 Gy to Myc-CaP tumors.

Antibody treatments

All antibodies were administered at 200 µg intraperitoneally. An anti-PD-1 hybridoma (clone G4) was given as a gift by Lieping Chen. Anti-PD-1 antibody was produced by Envigo (Madison, WI). Anti-PD-1 was administered intraperitoneally either on day 0 or days 0, 3, and 6 following TRT. Anti-PD-L1 antibody (BioXCell, Lebanon NH, BE0101) was given on days 0, 3, and 6 following TRT. Anti-CTLA-4 IgG2b was purchased from BioXCell (BP0164), while anti-CTLA-4 IgG2a was produced by Neoclone (Madison, WI) from a hybridoma provided by Bristol-Myers Squibb (New York City, NY). Anti-CTLA-4 antibodies were given on days 0, 3, and 6 following TRT. Armenian Hamster IgG (BioXCell BE0091) and Mouse IgG2a (BioXCell BP0085) were used as controls.

DEREG mice

Hemizygous male DEREG mice were implanted with TRAMP-C1 tumors as above then injected intraperitoneally on day −2 and day −1 before TRT with 1 µg diptheria toxin to transiently deplete Tregs. They were also treated with IgG or anti-PD-1 on day 0 as above.

Complete blood count

TRAMP-C1 (n=5 per group) and Myc-CaP (n=3 per group) tumor-bearing mice were treated with low-dose or high-dose TRT as above. Mice were then euthanized at several time points and blood was collected via cardiac puncture. Complete blood count (CBC) analysis was performed using a VetScan HM5 veterinary hematology analyzer (Abaxis, Union City, CA).

Flow cytometry

Mice were implanted with TRAMP-C1 or Myc-CaP tumors and treated with TRT as above. Tumors were collected at various time points following TRT then digested for 1–2 hours at 37° in mouse cell culture medium: RPMI 1640 with L-glutamine, 10% fetal calf serum (FCS), 200 U/mL Pen/Strep, 5% sodium pyruvate, 5% HEPES, and 50 µM β-MeOH supplemented with 2 mg/mL collagenase, 0.2 mg/mL DNAse I, and 1 tablet protease inhibitor (Sigma-Aldrich, St. Louis, MO, 11697498001) per 50 mL digest solution. Digests were then passed through 100 µm screens. Next, 5 million cells were plated and Fc blocked (BD, Franklin Lakes, NJ, 553142) for 20 min at 4°C. Cells were then stained for 30 min at 4°C with the viability dye Ghost Dye Red 780 (Tonbo 13-0865 T100) and up to 12 of the following antibodies: CD11b-BB515 (BD 564454), CD25-BB700 (BD 566498), GR-1-PE-CF594 (BD 562710), CD3-PE-Cy7 (eBiosciences Thermo Fisher Scientific, Waltham, MA 25-0031-82), MHCII-BV421 (Biolegend San Diego, CA 107632), CD45-BV510 (BD 563891), CD4-BV605 (Biolegend 100451), CD19-BV711 (BD 563157), CD11c-APC (BD 550261), CD8-AF700 (100730), CD44-AF488 (Biolegend 103016), CD45-PerCP-Cy5.5 (Biolegend 103132), KLRG-1-PE (Biolegend 138408), CD69-PE-CF594 (BD 562455), CD62L-BV510 (Biolegend 104441), CD103-BV605 (Biolegend 121453), CD27-BV785 (Biolegend 124241), CD4-APC-Cy7 (Biolegend 561830), LAG-3-BB515 (BD 564672), CD3-PerCP-Cy5.5 (BD 561108), TIGIT-PE (Biolegend 156104), TIM-3-PE-Dazzle594 (Biolegend 134014), CTLA-4-PE-Cy7 (Biolegend 106314), VISTA-BV421 (Biolegend 150212), PD-1-BV711 (BD 748265), CD137-APC (Biolegend 106110), CD11c-BB515 (BD 565586), MHCII-PerCP-Cy5.5 (BD 562363), CD137L-PE (Biolegend 10705), H-2Db-PE-Dazzle594 (Biolegend 111522), CD155-PE-Dazzle594 (Biolegend 131516), GR-1-PE-Cy7 (BD 552985), PD-L1-BV605 (Biolegend 124321), CD86-BV711 (BD 740709), Gal-9-APC (Biolegend 137912), and CD11b-AF700 (BD 557960)

Cells were then fixed and permeabilized with the eBioscience Foxp3/Transcription Factor Staining Buffer Set overnight at 4°C (Thermo Fisher 00-5523-00). Cells were then stained with intracellular antibodies for 30 min at 4°C: FoxP3-PE (Thermo Fisher 12-5773-82), Ki67-BV421 (BD 562899).

Stained and fixed cells were then resuspended in 90% FCS and 10% DMSO then frozen at −80°C until ready for analysis. Flow cytometry was performed on a Thermo Fisher Attune NxT cytometer and data were analyzed using FlowJo V.10. Gates were set according to fluorescence minus one controls. Gating strategies are shown in online supplemental figures 1–4.

In vitro studies
Treg suppression assays

Spleens were harvested from wild-type C57/BL6 mice and passed through 100 µm screens. CD8 +T cells were isolated from splenocytes via immunomagnetic negative

selection (StemCell Vancouver, BC, Canada, 19853), then labeled with PKH26 (Sigma PKH26GL-1KT) or carboxyfluorescein succinimidyl ester (CFSE, Biolegend 423801) according to the manufacturer's instructions. Spleens and tumors were collected from TRAMP-C1 tumor-bearing mice 7 days following either no treatment or high-dose TRT treatment and processed into single cell suspensions as above. Tregs were then isolated from these tissues using the EasySep Mouse CD4 +CD25+Regulatory T Cell Isolation Kit II (StemCell 18783). 1×10^5 labeled CD8 +T cells were cultured together with Tregs at a 1:1 or 1:10 ratio of Tregs to CD8 +T cells. CD8 +T cells were stimulated with anti-CD3/anti-CD28 coated beads (Thermo Fisher 11 456D) at a ratio of 2 beads per CD8 +T cell. Cells were cultured with 30 units/mL of human IL-2 for 72 hours in 96-well plates before analysis via flow cytometry.

To test the effects of PD-1/PD-L1 signaling on Treg suppressive ability, M-450 Tosylactivated beads (Thermo Fisher Scientific 14013) were coated with anti-CD3, anti-CD28, and PD-L1 Fc (R&D Systems Minneapolis, MN) or Mouse IgG2a control according to the manufacturer's instructions. Briefly, 8×10^7 beads were incubated in 0.1 M sodium phosphate buffer with 40 µg of total protein comprised of 10% anti-CD3 (Biolegend 100339), 10% anti-CD28 (Biolegend 102115), and 80% IgG for CD3/28/IgG beads, or 10% PD-L1 and 70% IgG for CD3/28/PD-L1 beads. Beads were washed three times with PBS+0.1% BSA and 2 mM EDTA before use. CD3/28/IgG or CD3/28/PD-L1 beads were added to cultures containing labeled CD8 +T cells and Tregs in place of ready-made anti-CD3/anti-CD28 beads. Anti-PD-1 or IgG was added to the culture at 5 µg/mL. Cells were cultured as before for 72 hours then cells were analyzed for proliferation via flow cytometry.

Cd8+ T cell functional assay

TRAMP-C1 tumor cell suspensions were obtained from untreated or TRT-treated mice as above. CD8 +T cells were then isolated using immunomagnetic separation then stimulated with anti-CD3/anti-CD28 beads for 48 hours. The plate was frozen at −80 until radioactive cells had decayed to background level, then media was analyzed for IFNγ secretion via ELISA.

ELISA

ELISA was performed as previously described.[41] Briefly, plates were coated overnight at 4°C with anti-mouse IFNγ antibody (BD #551216), then blocked with PBS/1% BSA before adding standards (BD #554587) and supernatants and incubating the plate overnight at 4°C. The next day, biotin-conjugated anti-mouse IFNγ antibody was added (BD #554410), followed by avidin-HRP (BioRad Hercules, CA, 170-6528), and TMB Substrate (Kirkegaard and Perry, Gaithersburg, MD, 50-76-01), stopped with 1N HCl, and read at OD^{450}.

Statistical analysis

Time course CBC and flow cytometry data were analyzed via two-way analysis of variance (ANOVA), followed by pairwise testing and p value adjustment according to the Benjamini-Hochberg (BH) procedure when comparing all conditions to baseline or planned contrasts when comparing only two conditions at each time point. For experiments in which there was not an untreated control for every time point, all untreated control data (day 0 and day 29) was pooled, then each TRT-treated condition was compared with this control. Flow cytometry data collected at a single time point and ELISA data were analyzed via one-way ANOVA followed by pairwise testing and BH adjustment. Tumor growth data were analyzed by fitting a linear mixed-effects model followed by pairwise testing and BH adjustment. Survival data were tested via the log rank test followed by pairwise testing and BH adjustment. All data analysis was performed in R V.4.0.2.

RESULTS

⁹⁰Y-NM600 could be given at safe doses but was not curative in prostate tumor models

We studied the effects of ⁹⁰Y-NM600 on two established murine prostate tumor models. Specifically, we used the TRAMP-C1 and Myc-CaP models to see if our results could be reproduced across tumors with different growth rates, genetic backgrounds, driver mutations, ⁹⁰Y-NM600 uptake, and baseline immune infiltration. To determine whether ⁹⁰Y-NM600 exhibited favorable therapeutic ratios in these models, we implanted tumor cells and waited until they reached a volume of approximately 100–200 mm³ before administering ⁸⁶Y-NM600 via tail vein. We then determined longitudinal tumor and normal tissue distribution via serial PET/CT imaging (online supplemental figure 5A)[34] to estimate ⁹⁰Y-NM600 dosimetry. We estimated that we could deliver a comparable or higher dose to the tumor than to all normal tissues in each experimental system (figure 1A,B). High liver dose was expected given that NM600 is hepatically cleared. Given our previous finding that up to 250 µCi of ⁹⁰Y-NM600 can be safely administered before inducing severe bone marrow toxicity,[36] we evaluated two dose levels of ⁹⁰Y-NM600: 50 µCi of injected activity (low dose) and 250 µCi of injected activity (high dose). We estimated that low-dose TRT delivered 1–2 Gy to TRAMP-C1 and 4–5 Gy to Myc-CaP tumors, while high-dose TRT delivered 5–6 Gy to TRAMP-C1 tumors and 16–20 Gy to Myc-CaP tumors. We injected ⁹⁰Y-NM600 intravenously into tumor-bearing mice at the two doses and collected blood at several timepoints, then assessed for changes in peripheral blood counts via CBC. We found that both low-dose and high-dose ⁹⁰Y-NM600 could be administered without severe bone marrow toxicity. There was a transient drop in white cell counts, lymphocytes, and hemoglobin in the TRAMP-C1 model which was more pronounced following high-dose administration but resolved by the end of the study period (figure 1C–F). We found
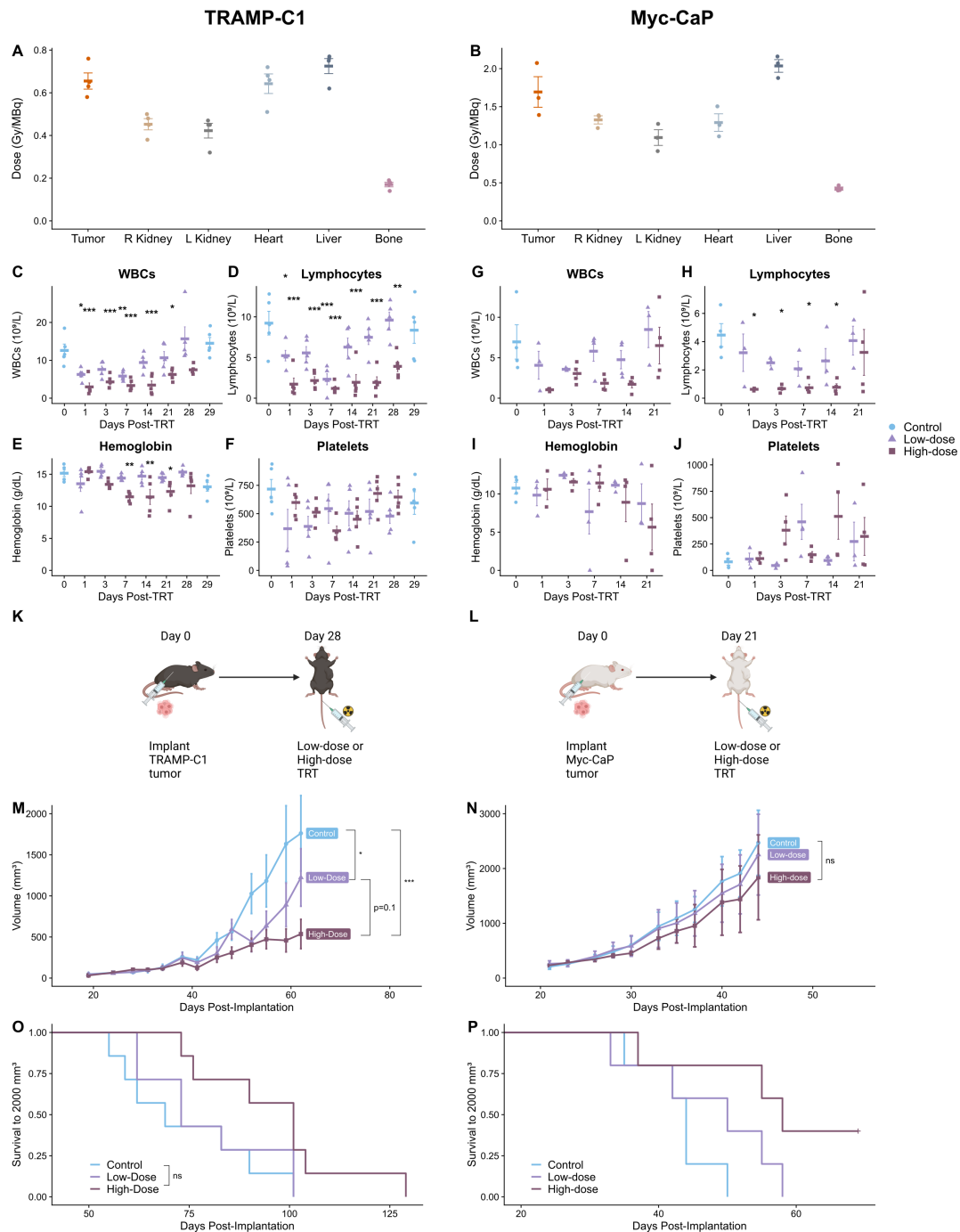
Figure 1 ^{90}Y-NM600 could be given at safe doses but was not curative in prostate tumor models. Tumor-bearing mice were injected with ^{86}Y-NM600 and imaged via serial PET/CT at several time points as shown in online supplemental figure 5A.[34] Normal tissue and tumor dosimetry were then estimated in (A) TRAMP-C1 (n=4 mice per group) and (B) Myc-CaP (n=3 mice per group) as previously published.[34] Tumor-bearing mice were treated with a single intravenous administration of ^{90}Y-NM600. Blood was then collected at various timepoints. (C–F) Complete blood count data in untreated, low-dose treated, and high-dose TRT-treated animals (n=5 per group) bearing TRAMP-C1 tumors. (G–J) Corresponding complete blood count data in TRT-treated animals (n=3 per group) bearing Myc-CaP tumors. Mice were given either no treatment, low-dose TRT or high-dose TRT as shown in the study schemas for (K) TRAMP-C1 tumor-bearing mice (n=7 per group) or (L) Myc-CaP-tumor-bearing mice (n=5 per group). Growth curves are shown for (M) TRAMP-C1and (N) Myc-CaP tumors (n=5 per group). Lightning bolt symbols indicate the day that TRT treatment was administered. (O, P) Kaplan-Meier curves depicting survival (time to a tumor size of 2000 mm^3 or death) in mice from M and N, respectively. *P<0.05, **p<0.01, ***p<0.001 compared with untreated controls. Error bars represent mean±SE. Tumor growth curves were compared using linear mixed-effects model followed by pairwise testing and BH adjustment. Kaplan-Meier curves were compared using the log-rank test followed by pairwise testing and BH adjustment. Results shown are from one experiment and are representative of two independent experiments (shown in online supplemental figure 5D–G). BH, Benjamini-Hochberg; ns, not significant; TRT, targeted radionuclide therapy; PET, positron emission tomography.

similar results in the Myc-CaP model, though only the decrease in lymphocytes reached statistical significance (figure 1G–J). We observed a trend toward an absorbed dose-dependent effect on tumor growth in both models. In the TRAMP-C1 model, both low-dose and high-dose TRT significantly slowed tumor growth compared with control. There was a trend toward slower tumor growth in the high-dose treated mice than in low-dose treated mice, though this was not significant (p=0.1). There was no significant improvement in survival in either the low-dose (p=0.81; HR 0.74, 95% CI 0.26 to 2.13) or high-dose conditions (p=0.06; HR 0.28, 95% CI 0.09 to 0.91). In the Myc-CaP model, there was no significant difference in tumor growth rate in either the low-dose or the high-dose condition. There was significantly improved survival in the high-dose treatment arm in the Myc-CaP model (p=0.038; HR 0.13, 95% CI 0.02 to 0.73) but not in the low-dose treatment arm (p=0.378; HR 0.42, 95% CI 0.10 to 1.77), and no significant difference between the low-dose and high-dose arms (p=0.25) High-dose ^{90}Y-NM600 was not sufficient to elicit regression of either tumor type (figure 1K–P, online supplemental figure 5B–G).

^{90}Y-NM600 increased CD8+ T cell infiltration into prostate tumors but also increased checkpoint molecule expression

Having established that ^{90}Y-NM600 TRT could be administered safely, we next investigated its effects on the tumor immune microenvironment via flow cytometry of TRT-treated tumors. We found that TRT caused an initial decline in CD8 +T cell numbers, but with high-dose treatment, T cells recovered and exceeded baseline levels on day 14 post-TRT in the TRAMP-C1 model (figure 2A, p=0.006). We observed the same trend in the Myc-CaP model, though the increase in CD8 +T cells was not significant (online supplemental figure 6A). High-dose TRT also increased activation of CD8 +T cells in TRAMP-C1 tumors on day 3, with increases in CD69 (p<0.001), and CD137 (p=0.004) expression (figure 2B). Further immunophenotyping of the CD8 +T cell compartment revealed an early increase in effector memory CD8 +T cells after TRT administration, with no increase in central memory, resident memory, or short-lived effector cells (figure 2C). Examining checkpoint molecule expression on CD8 +T cells recovering following TRT treatment revealed elevated expression of PD-1, CTLA-4, LAG-3, and VISTA in high-dose treated tumors (figure 2D). Checkpoint molecule expression followed similar patterns in the Myc-CaP model, though only CTLA-4 expression was significantly elevated over baseline (online supplemental figure 6B–D). Finally, we measured PD-L1 expression and found an increase in PD-L1 expression on day 1 (p=0.009) and 3 (p=0.005) on CD11b+Gr-1+myeloid derived suppressor cells (MDSCs) treated with high-dose TRT. Dendritic cells (DCs) from high-dose treated mice showed a similar but non-significant increase in PD-L1 expression at day 3 (p=0.052), while no increase was seen on tumor cells (figure 2E). In contrast, in the Myc-CaP model, tumor cells showed PD-L1 expression peaking at Day 4 in both the low-dose (p=0.003) and high-dose (p<0.001) conditions (online supplemental figure 6E). Taken together, these

data suggest that ^{90}Y-NM600 may be capable of driving activated CD8 +T cell infiltration into the tumor microenvironment, but over time these T cells begin to express high levels of immune checkpoint molecules while myeloid cells express increased PD-L1. Our findings also demonstrated that high-dose ^{90}Y-NM600 exerted a stronger antitumor effect, and also elicited a concomitantly stronger immune response than low-dose ^{90}Y-NM600.

Adding PD-1 blockade to ^{90}Y-NM600 TRT did not improve antitumor efficacy

Due to the increased PD-1 expression on CD8 +T cells and PD-L1 expression on myeloid cells following TRT, we hypothesized that blockade of the PD-1/PD-L1 axis in combination with TRT would further improve antitumor efficacy. To test this, we implanted prostate tumors and treated with a single administration of ^{90}Y-NM600 at the two dose levels as before, together with a single treatment with either IgG or anti-PD-1 on the same day (figure 3A,B). We then followed mice for tumor growth. However, in the TRAMP-C1 model, we unexpectedly observed an attenuation in antitumor response in the TRT+anti-PD-1 condition compared with TRT+IgG (p=0.02, figure 3C). In the Myc-CaP model, we observed no added benefit to combining anti-PD-1 and TRT (figure 3D, online supplemental figure 7D). We further tested delivering anti-PD-1 therapy 6 days after high-dose TRT, on days 0, 3, and 6 following high-dose TRT, and giving anti-PD-L1 therapy on days 0, 3, and 6 following high-dose TRT in TRAMP-C1 tumor-bearing mice; we observed either no improvement in antitumor efficacy or a reduction in the efficacy of TRT (online supplemental figure 7A,C). Similarly, anti-PD-1 therapy did not augment antitumor efficacy when combined with low-dose TRT (online supplemental figure 7B,C).

Combined ^{90}Y-NM600 TRT and PD-1 blockade increased intratumoral Treg frequency while reducing effector memory CD8+ T cell populations

To investigate the mechanism of this unexpected finding, we performed a similar study as in figure 3A but collected tumors at several timepoints following treatment for evaluation of the immune cell composition via flow cytometry. We found that the addition of PD-1 blockade to TRT was associated with increased Treg frequency at Day 8 compared with IgG +TRT (p=0.04), with no changes in the frequency of MDSCs (figure 4A,B). Though it has been reported that certain clones of anti-mouse anti-PD-1 antibodies can deplete CD8 +T cells through Fc gamma receptor binding,[42] we found an increase in all CD8 +T cells with the addition of anti-PD-1 at Day 14 (p=0.005, figure 4C). However, there was a specific decrease in effector memory cells at day 3 when anti-PD-1 was added (p=0.02, figure 4D). The other CD8 +T cell memory subsets did not significantly differ between the anti-PD-1 and IgG conditions (figure 4E–G).
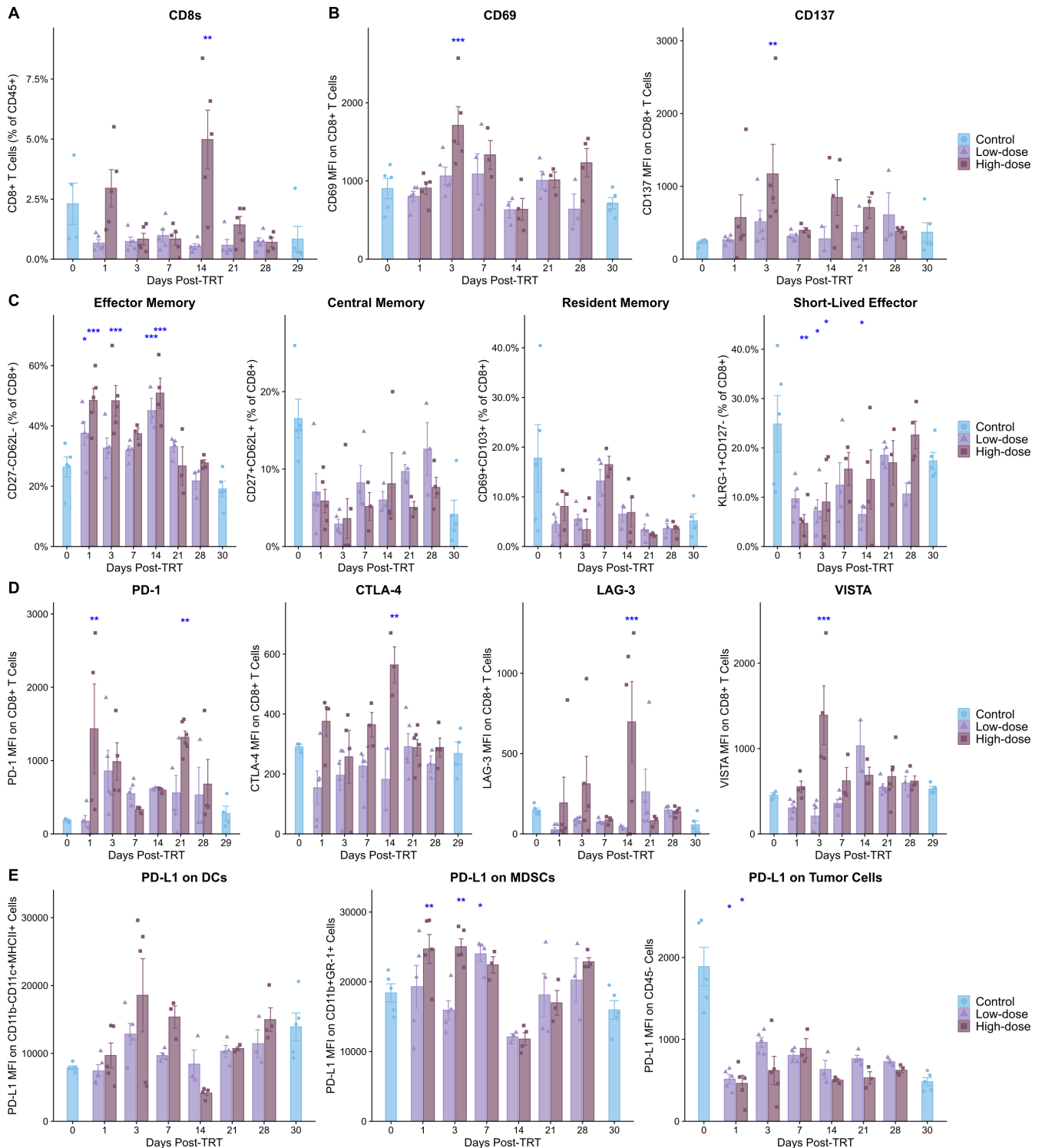
Figure 2 ^{90}Y-NM600 increased CD8 +T cell infiltration into prostate tumors but also increased checkpoint molecule expression. TRAMP-C1 tumors were collected from mice (n=5 per group) at several time points following no treatment (control), low-dose TRT, or high-dose TRT, digested, and evaluated for cellular composition by flow cytometry. Shown are: (A) CD3 +CD8+T cells as a percentage of CD45 +cells. (B) CD69 (left) and CD137 (right) median fluorescence intensity (MFI) on CD8 +T cells. (C) Percent of CD8 +T cells bearing markers for effector memory (CD44 +CD27-CD62L-), central memory (CD44 +CD27+CD62L+), resident memory (CD44 +CD69+CD103+) or short-lived effector (KLRG-1 +CD127-) cell phenotypes. (D) MFI of PD-1, CTLA-4, LAG-3, and VISTA on CD8 +T cells (E) PD-L1 MFI on dendritic cells (CD11b-CD11c+MHCII+ cells), myeloid-derived suppressor cells (MDSCs; CD11b+Gr-1+), and tumor cells (CD45-). *P<0.05, **p<0.01, *** p<0.001 compared with untreated controls via two-way ANOVA with Benjamini-Hochberg adjustment of pairwise tests. To perform pairwise testing, untreated controls were pooled then compared with each TRT-treated group. Error bars represent mean±SE. Results shown are from one experiment and are representative of two independent experiments. ANOVA, analysis of variance; DCs, dendritic cells; TRT, targeted radionuclide therapy.
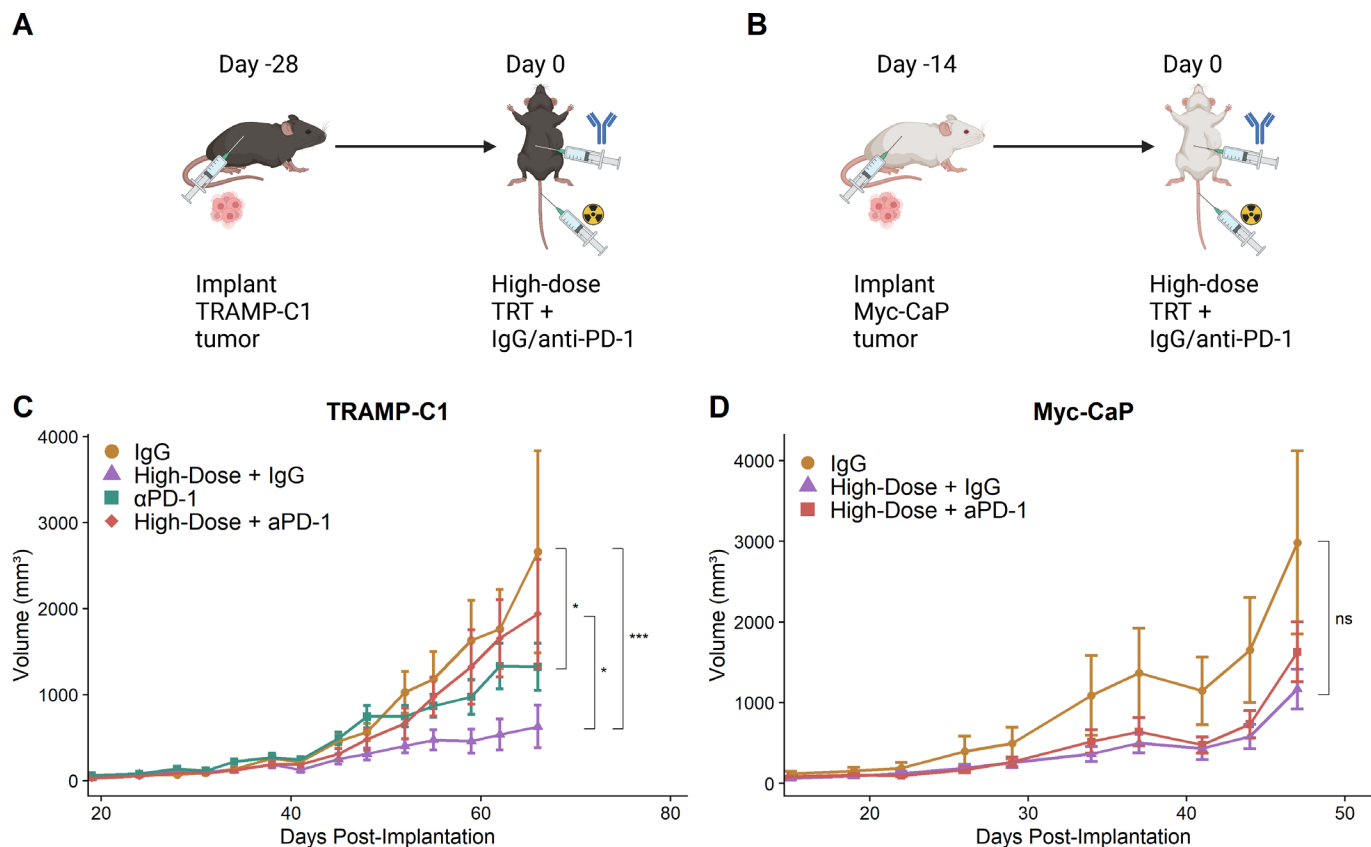
Figure 3 Adding PD-1 blockade to ^{90}Y-NM600 TRT did not improve antitumor efficacy. Tumor-bearing mice were treated with high-dose TRT and a single 200 µg dose of anti-PD-1 or IgG given on the same day. Schemas are shown for studies done in the (A) TRAMP-C1 model and (B) Myc-CaP model. Tumor growth curves are shown in the (C) TRAMP-C1 (n=7 per group) and (D) Myc-CaP models (n=8 per group). *P<0.05, ***p<0.001 via linear mixed-effects model with Benjamini-Hochberg adjustment of pairwise testing. Error bars represent mean±SE. Results shown are from one experiment and are representative of two independent experiments. TRT, targeted radionuclide therapy.

^{90}Y-NM600 TRT with PD-1 blockade increased suppressive activity of Tregs while decreasing activity of CD8+ T cells

Based on these findings and previous reports,[43] we hypothesized that PD-1 blockade following TRT may result in increased suppressive activity by Tregs, resulting in an impaired antitumor response. We first examined whether ^{90}Y-NM600 alone affected Treg or CD8 +T cell function. To assess Treg function, we isolated Tregs from TRAMP-C1 tumor-bearing mice that received either no treatment or TRT 1 week prior, and then cultured them in the presence of wild-type CD8 +T cells labeled with a membrane-incorporating dye. We found that Tregs from the spleens and tumors of TRAMP-C1 tumor-bearing mice were equally effective at suppressing CD8 +T cell proliferation whether or not they had received radiation (figure 5A,B). To measure CD8 +T cell function, we collected CD8 +T cells from TRAMP-C1 tumors 1 week following no treatment or TRT, treated them with anti-CD3/anti-CD28 stimulation, and then measured IFNγ secretion. We found that unlike untreated CD8 +T cells, TRT-treated CD8 +T cells did not secrete greater IFNγ than background (figure 5C). These data demonstrated that ^{90}Y-NM600 at these doses left Tregs functional while rendering CD8 +T cells dysfunctional. We next measured

PD-1 expression on CD8 +T cells and Tregs in TRAMP-C1 tumors, and found that in non-TRT treated tumors, Tregs had at least twofold greater expression of PD-1 on days 3, 7, and 14 (figure 5D). In TRT-treated tumors, there was an induction in PD-1 expression on CD8 +T cells at day 14 as shown earlier, but at day 3 and day 7, Tregs continued to express higher levels of PD-1 (figure 5D). Moreover, looking at numbers of PD-1 +T cells, we found that there were fivefold more PD-1 +Tregs on day 7 compared with PD-1 +CD8 s in TRT-treated tumors (figure 5E). Taken together, these data suggested that Tregs were the dominant source of PD-1 expression in the murine prostate microenvironment. To evaluate whether PD-1 blockade affected Treg function, we again used an in vitro co-culture assay with labeled CD8 +T cells from naïve mice and Tregs from TRAMP-C1 tumor-bearing mice. When anti-PD-1 antibody was added to the in vitro culture with PD-L1 coated beads in the absence of Tregs, we observed increased proliferation compared with when IgG was added, as expected (figure 5F, p=0.02). By contrast, when Tregs were present, adding anti-PD-1 resulted in decreased proliferation compared with IgG, indicating greater suppression by Tregs (Figure 5G,H, p=0.001).
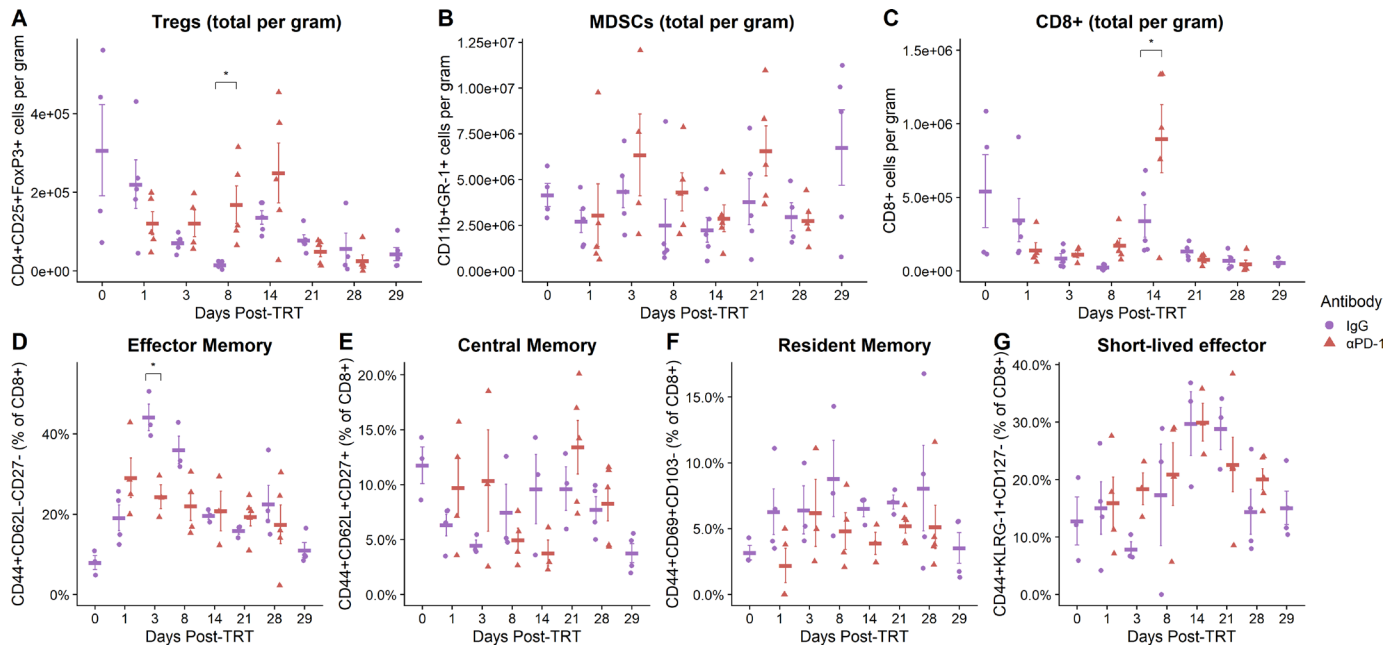
Figure 4 Combined ^{90}Y-NM600 TRT and PD-1 blockade increased intratumoral Treg frequency while reducing effector memory CD8 +T cell populations. TRAMP-C1 tumor-bearing mice (n=5 per group) were given either IgG treatment alone (Day 0 and 29), TRT+IgG, or TRT+anti-PD-1. Antibody treatments were administered on the same day as the TRT. Flow cytometry data from tumors harvested at various timepoints following treatment are shown. (A) Absolute number of Tregs (CD4 +CD25+FoxP3+) per gram of tumor tissue. (B) Absolute number of MDSCs (CD11b+Gr-1+) per gram of tumor tissue. (C) Absolute number of CD3 +CD8+T cells per gram of tumor tissue. Percent of CD8 +T cells-bearing markers for (D) effector memory (CD44 +CD27-CD62L-), (E) central memory (CD44 +CD27+CD62L+), (F) resident memory (CD44 +CD69+CD103+) cell phenotype, or (G) short-lived effector (KLRG-1 +CD127-). *P<0.05 via two-way ANOVA with planned contrasts between IgG and anti-PD-1 groups at each timepoint. Error bars represent mean±SE. Results shown are from one experiment and are representative of two independent experiments. ANOVA, analysis of variance; MDSCs, myeloid derived suppressor cells; TRT, targeted radionuclide therapy.

Treg depletion improved antitumor response with anti-PD-1 + ^{90}Y-NM600

Having determined that Treg activation by anti-PD-1 was likely mediating the lack of efficacy of the TRT and anti-PD-1 combination, we next tested whether depleting Tregs in vivo would improve antitumor efficacy. It has been previously reported that an anti-CTLA-4 IgG2a isotype antibody effectively depletes intratumoral Tregs, unlike the IgG2b isotype.[44] We treated TRAMP-C1 tumor-bearing mice with either IgG, TRT+anti-PD-1+anti-CTLA-4 IgG2a or TRT+anti-PD-1+anti-CTLA-4 IgG2b as shown in figure 6A, then collected tumors for flow cytometry 1 week following TRT. We confirmed that the combination of TRT, anti-PD-1, and anti-CTLA-4 IgG2a did deplete Tregs in TRAMP-C1 tumors, unlike the TRT, anti-PD-1, and anti-CTLA-4 IgG2b combination (p=0.001, figure 6B). TRAMP-C1 tumors treated with TRT, anti-PD-1, and the Treg-depleting anti-CTLA-4 antibody also had greater numbers of effector memory CD8 +T cells (figure 6C). When we treated mice-bearing TRAMP-C1 tumors with anti-PD-1+TRT and followed for tumor growth, the addition of the depleting antibody, but not the non-depleting antibody, resulted in improved antitumor response compared with TRT alone (p=0.047) (figure 6D,E, online supplemental figure 8A). In the Myc-CaP model, the Treg-depleting anti-CTLA-4 antibody

alone was sufficient to regress most of the tumors, making it difficult to assess the effect of Treg depletion on the TRT+anti-PD-1 combination (online supplemental figure 8B). To evaluate the effects of conditional Treg depletion without the use of CTLA-4 blockade, we used DEREG mice.[45] We verified that administration of diptheria toxin to DEREG mice resulted in near complete depletion of Tregs (online supplemental figure 9A,B). We similarly observed significantly improved antitumor efficacy with the anti-PD-1+TRT regimen compared with control when Tregs were depleted (p=0.039), but not in the presence of Tregs (online supplemental figure 9C,D).

DISCUSSION

There has been increasing interest in TRT treatments for prostate cancer as well as combination radiation and immunotherapy approaches. However, there are limited preclinical data describing the effects of TRT on immune populations within tumors and how best to combine it with checkpoint blockade. In this study, we evaluated the effects of ^{90}Y-NM600 TRT on the murine prostate tumor microenvironment alone and in combination with PD-1 blockade. Our main conclusions were as follows: (1) ^{90}Y-NM600 can be given at safe doses to murine prostate tumors and elicits a moderate antitumor effect; (2)
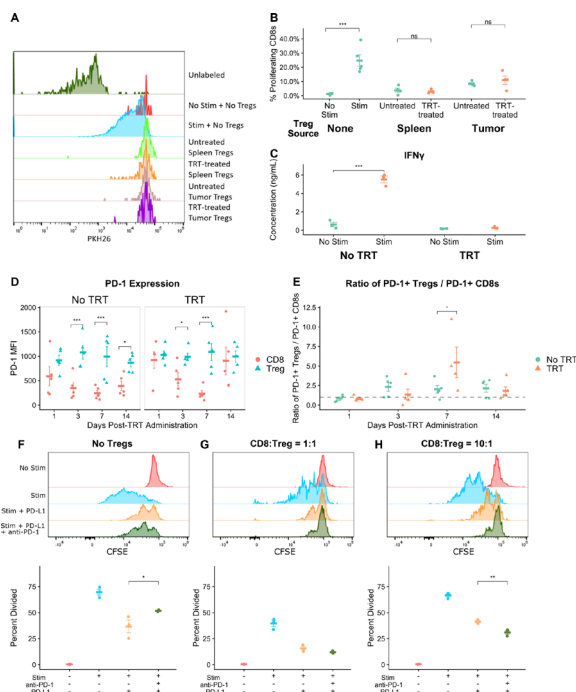
Figure 5 ^{90}Y-NM600 TRT with PD-1 blockade increased suppressive activity of Tregs while decreasing activity of CD8 +T cells. CD8 +T cells were harvested from WT mice and labeled with PKH26. Labeled CD8s were cultured alone or co-cultured with Tregs harvested from either the spleen or tumor of TRAMP-C1 tumor-bearing mice that had received no treatment or high-dose TRT 7 days prior. Cells were collected after 72 hours of culture in the presence of anti-CD3/anti-CD28 beads and analyzed via flow cytometry for PKH26 loss as an indicator of proliferation. (A) Representative flow cytometry data (B) Quantification of A. Shown is the percent of CD8 +T cells with proliferation greater than background. (C) CD8 +T cells were harvested from TRAMP-C1 tumor-bearing mice 7 days following no treatment or high-dose TRT treatment, and then cultured for 48 hours with anti-CD3/anti-CD28-coated beads. Shown is IFNγ concentration from supernatants of this culture measured via ELISA. TRAMP-C1 tumor-bearing mice (n=5 per group) were treated with TRT then harvested at several timepoints following no treatment or high-dose TRT treatment as in figure 2A. Flow cytometry showing (D) PD-1 MFI on CD8 +T cells (red) and Tregs (blue) in untreated tumors (left) and TRT-treated tumors (right), and (E) the ratio of the number of PD-1 +Tregs to the number of PD-1 +CD8+T cells. CD8 +T cells were harvested from WT mice and labeled with CFSE. Labeled CD8s were cultured alone or co-cultured with Tregs harvested from the spleens of untreated TRAMP-C1 tumor-bearing mice at the indicated ratios (control without Tregs F, 1:1 ratio G, 10:1 ratio (H) of CD8s to Tregs. Cells were collected after 72 hours of culture in the presence of anti-CD3/anti-CD28/IgG or anti-CD3/anti-CD28/PD-L1 beads, with anti-PD-1 or IgG in the media and analyzed via flow cytometry for CFSE loss as an indicator of proliferation. Top panels are representative flow cytometry data. Bottom panels depict quantification of the top panels using the percent divided metric (FlowJo proliferation analysis software). *P<0.05, **p<0.01, ***p<0.001. Error bars represent mean±SE. Results shown are representative of two independent experiments. ns, not significant; TRT, targeted radionuclide therapy; CFSE carboxyfluorescein succinimidyl ester.

^{90}Y-NM600 has complex effects on immune populations within the tumor microenvironment, with different cell types having varying susceptibilities to radiation; (3) combination ^{90}Y-NM600 and PD-1 blockade is ineffective in these models due to the persistence of Tregs and the activating effects of PD-1 blockade on this population; (4) TRT could potentially predispose Treg-rich tumors to 'hyperprogression' following PD-1 blockade and (5) careful evaluation of the effects of other radioisotopes or TRT agents on the tumor microenvironment could be crucial for successful combination with checkpoint blockade.

This work is the first to demonstrate that ^{90}Y-NM600 can be safely used in murine prostate tumors. We estimated that dose to the tumor was higher or comparable to dose delivered to organs at risk. Our previous work has demonstrated that although other organs, particularly the liver, receive some radiation dose, no clinically significant effects were seen on blood chemistry or histology at the tested levels of injected activity.[36] There was some evidence of bone marrow toxicity at higher doses as seen via CBC, but all cytopenias resolved within the study period. We found that at this maximally tolerated dose, single-agent ^{90}Y-NM600 treatment was able to slow tumor growth significantly, though this was not curative.

Despite the relative lack of systemic toxicity it induced, ^{90}Y-NM600 treatment resulted in considerable changes in the prostate tumor immune microenvironment. Myeloid cells and DCs from TRT-treated tumors had increased expression of PD-L1. Additionally, CD8 +T cell infiltration increased after TRT. Soon after treatment, these CD8 +T cells expressed greater levels of activation markers and displayed evidence of induction of an effector memory response, but later expressed higher levels of checkpoint molecules consistent with an exhausted state. In fact, we showed that CD8 +T cells were dysfunctional 1 week following TRT. Nearly all preclinical studies showing that radiation potentiates a CD8 +T cell response have used EBRT. Unlike EBRT, ^{90}Y-NM600 TRT results in continuous delivery of radiation to the tumor over several days. This could potentially result in prolonged dysfunction of CD8 +T cells. The exquisite sensitivity of CD8 +T cells to radiation may be a barrier to overcome for future attempts to combine TRT and immune-based treatments relying on this cytotoxic population. Proper sequencing of the two treatments may be essential for the efficacy of this combination.

By contrast, Tregs did not lose suppressive function following ^{90}Y-NM600 treatment. Tregs have been shown to be particularly radioresistant compared with other lymphocytes, possibly due to increased expression of anti-apoptotic factors such as BCL-2 and GITR.[46–48] This persistence of Tregs likely explains why our results demonstrated an attenuation in the antitumor effect of ^{90}Y-NM600 when PD-1 blockade was used. We showed that Tregs were the highest PD-1-expressing cell type in the tumor, even following TRT. Therefore, when PD-1 was blocked, the suppressive ability of the Tregs was enhanced,
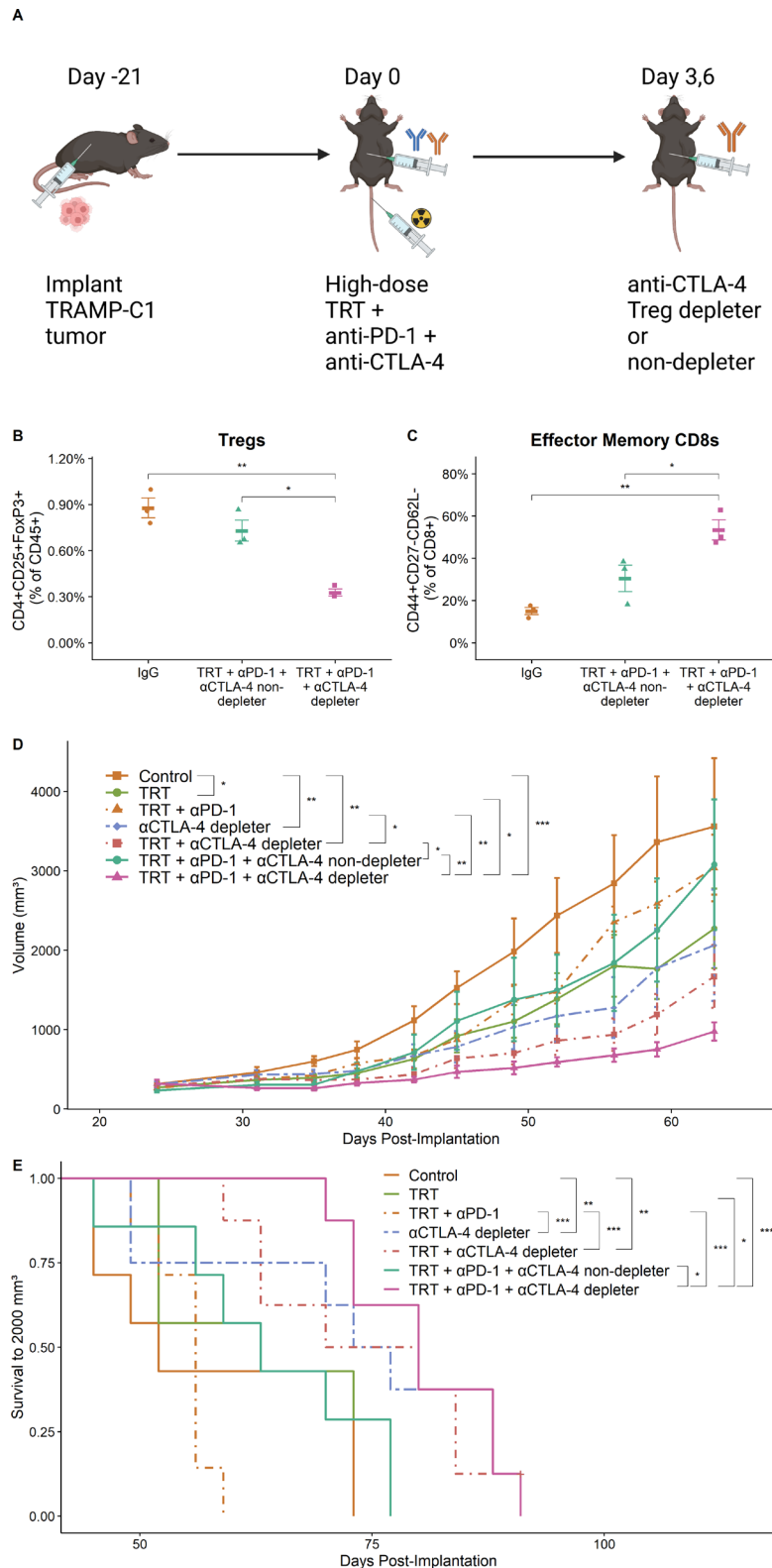
Figure 6 Treg depletion improved antitumor response with anti-PD-1 + ^{90}Y-NM600. Tramp-C1 tumors were collected from animals (n=3 per group) treated with IgG alone, TRT+anti-PD-1+non Treg depleting anti-CTLA-4 (non-depleter), or TRT+anti-PD-1+Treg-depleting anti-CTLA-4 (depleter). Anti-PD-1 was given on Day 0 and anti-CTLA-4 was given on days 0, 3, and 6 following TRT. Each antibody treatment used 200 µg antibody delivered i.p. (A) Study schema. Tumors were digested and evaluated by flow cytometry 7 days after TRT for (B) Tregs (CD4 +CD25+FoxP3+) cells as a percent of CD45 +cells, and (C) Effector memory cells (CD44 +CD27-CD62L-) as a percent of CD8 +T cells. TRAMP-C1 tumor-bearing mice (n=7 per group) were treated with high-dose TRT, anti-PD-1, and anti-CTLA-4 as before and followed for (D) tumor growth and (E) survival to a tumor volume of 2000 mm³. *P<0.05, **p<0.01, ***p<0.001. Error bars represent mean±SE. Results shown are from one experiment and are representative of two independent experiments. TRT, targeted radionuclide therapy.

resulting in suppression of the effector memory CD8 +T cell response and a paradoxically impaired antitumor response. In our data, we observed that mice treated with TRT and PD-1 blockade had a lower overall number of Tregs than the untreated control, but significantly greater Treg numbers than in the TRT alone group at day 8. There were similar trends at day 3 and day 14, though these did not meet statistical significance. This finding could indicate that altering the timing of anti-PD-1 administration could result in different effects. These changes in Treg numbers are consistent with the observation that Tregs are relatively (though not completely) radioresistant and that PD-1 blockade increases their activity. Due to these effects, the combination of anti-PD-1 and ^{90}Y-NM600 was only effective in vivo when Tregs were absent.

Recently, there have been several reports of 'hyperprogression' following anti-PD-1 therapy in a subset of patients.[49 50] This pattern of progression is characterized by acceleration of the tumor growth rate and worsened overall survival.[51] Initial evidence suggested that hyperprogression may have a genetic component.[50] Further clinical and preclinical data have demonstrated that this phenomenon is likely in large part mediated by Tregs. Kamada *et al* showed that gastric cancers have abundant Tregs that express PD-1 at high levels. Patients with hyperprogressive disease had greater numbers of proliferating Tregs, while in vitro treatment of Tregs from tumors with anti-PD-1 resulted in greater suppressive activity.[52] Kang *et al* offered confirmatory evidence, showing that non-small cell lung cancer patients with hyperprogression had higher Treg frequencies than other patients.[53] Kumagai *et al* further showed that PD-1 expression balance on lymphocytes predicts outcomes following PD-1 blockade; patients with greater numbers of PD-1 +Tregs relative to PD-1 +CD8+T cells had significantly diminished survival.[43] Our data suggest that TRT may predispose tumors toward hyperprogression following PD-1 blockade by unfavorably modifying this PD-1 expression balance.

While this specific regimen of ^{90}Y-NM600 and anti-PD-1 therapy was not effective, this was not an exhaustive study of the combination of TRT and PD-1 blockade. It is possible that there could be differences in the effects of this combination therapy regimen in animals with different genetic backgrounds, though we did observe generally similar findings in both the C57BL/6/TRAMP-C1 and FVB/Myc-CaP models. ^{177}Lu and ^{225}Ac are other radioisotopes undergoing clinical study with longer half-lives and shorter path lengths, which may be better at treating small tumors than ^{90}Y and which may also result in different immunomodulatory effects. They could be more effective at causing DNA damage and immunogenic cell death, or temporarily depleting Tregs. This study focused on NM600 because of its ability to target many cancer types and utility in dosimetry-guided therapy studies. However, there are many other TRT agents in clinical use, such as PSMA-617, which may have greater selectivity for prostate tumors, enabling higher dose delivery, and thus could potentially combine more effectively with anti-PD-1 therapy. In future studies, we plan to investigate the effects of these other agents, higher-dose radiation given through EBRT or TRT, alternative radioisotopes, and potentially blockade of other checkpoint molecules.

This report demonstrates the importance of thoroughly investigating the effects of these TRT and immunotherapy regimens on the tumor microenvironment of immunocompetent mice to evaluate for proper choice of agent and timing. At the time of this writing, there are over 600 active clinical trials studying combinations of immunotherapy and radiation therapy, with several focused specifically on TRT and checkpoint blockade (eg, NCT05150236, NCT04946370, NCT03658447, and NCT03805594). Rational combination strategies based on preclinical data could be essential to prevent inferior results in these rapidly emerging clinical studies.

ORCID iDs
Ohyun Kwon http://orcid.org/0000-0002-0334-105X
Douglas G McNeel http://orcid.org/0000-0003-1471-6723

REFERENCES

1 Pons F, Herranz R, Garcia A, *et al*. Strontium-89 for palliation of pain from bone metastases in patients with prostate and breast cancer. *Eur J Nucl Med* 1997;24:1210–4.

2 Sartor O, Reid RH, Hoskin PJ, *et al*. Samarium-153-Lexidronam complex for treatment of painful bone metastases in hormone-refractory prostate cancer. *Urology* 2004;63:940–5.

3 Hoskin P, Sartor O, O'Sullivan JM, *et al*. Efficacy and safety of radium-223 dichloride in patients with castration-resistant prostate cancer and symptomatic bone metastases, with or without previous docetaxel use: a prespecified subgroup analysis from the randomised, double-blind, phase 3 ALSYMPCA trial. *Lancet Oncol* 2014;15:1397–406.

4 Bander NH, Milowsky MI, Nanus DM, *et al*. Phase I trial of [177] Lutetium-labeled J591, a monoclonal antibody to prostate-specific membrane antigen, in patients with androgen-independent prostate cancer. *J Clin Oncol* 2005;23:4591–601.

5 Tagawa ST, Milowsky MI, Morris M, *et al*. Phase II study of Lutetium-177–Labeled Anti-Prostate-Specific membrane antigen monoclonal antibody J591 for metastatic castration-resistant prostate cancer. *Clinical Cancer Research* 2013;19:5182–91.

6 Chen Y, Pullambhatla M, Foss CA, *et al*. 2-(3-{1-Carboxy-5-[(6-[18F] Fluoro-Pyridine-3-Carbonyl)-Amino]-Pentyl}-Ureido)-Pentanedioic Acid, [18F]DCFPyL, a PSMA-Based PET Imaging Agent for Prostate Cancer. *Clinical Cancer Research* 2011;17:7645–53.

7 Morris MJ, Rowe SP, Gorin MA, *et al*. Diagnostic performance of 18F-DCFPyL-PET/CT in men with biochemically recurrent prostate cancer: results from the CONDOR phase III, multicenter study. *Clinical Cancer Research* 2021;27:3674–82.

8 Pienta KJ, Gorin MA, Rowe SP, *et al*. A phase 2/3 prospective multicenter study of the diagnostic accuracy of prostate specific membrane antigen PET/CT with ^{18}F-DCFPyL in Prostate Cancer Patients (OSPREY). *J Urol* 2021;206:52–61.

9 Szabo Z, Mena E, Rowe SP, *et al*. Initial evaluation of [(18)F]DCFPyL for prostate-specific membrane antigen (psma)-targeted pet imaging of prostate cancer. *Mol Imaging Biol* 2015;17:565–74.

10 Eder M, Schäfer M, Bauder-Wüst U, *et al*. [68] Ga-Complex Lipophilicity and the Targeting Property of a Urea-Based PSMA Inhibitor for PET Imaging. *Bioconjug Chem* 2012;23:688–97.

11 Benešová M, Schäfer M, Bauder-Wüst U, *et al*. Preclinical evaluation of a tailor-made DOTA-conjugated PSMA inhibitor with optimized linker moiety for imaging and Endoradiotherapy of prostate cancer. *Journal of Nuclear Medicine* 2015;56:914–20.

12 Afshar-Oromieh A, Hetzheim H, Kratochwil C, *et al*. The theranostic PSMA ligand PSMA-617 in the diagnosis of prostate cancer by PET/CT: biodistribution in humans, radiation dosimetry, and first evaluation of tumor lesions. *J Nucl Med* 2015;56:1697–705.

13 Violet J, Jackson P, Ferdinandus J, *et al*. Dosimetry of [177] Lu-PSMA-617 in Metastatic Castration-Resistant Prostate Cancer: Correlations Between Pretherapeutic Imaging and Whole-Body Tumor Dosimetry with Treatment Outcomes. *J Nucl Med* 2019;60:517–23.

14 Sartor O, de Bono J, Chi KN. Lutetium-177–PSMA-617 for metastatic castration-resistant prostate cancer. *New England Journal of Medicine* 2021;0:null.

15 Formenti SC, Rudqvist N-P, Golden E, *et al*. Radiotherapy induces responses of lung cancer to CTLA-4 blockade. *Nat Med* 2018;24:1845–51.

16 Twyman-Saint Victor C, Rech AJ, Maity A, *et al*. Radiation and dual checkpoint blockade activate non-redundant immune mechanisms in cancer. *Nature* 2015;520:373–7.

17 Newton JM, Hanoteau A, Liu H-C, *et al*. Immune microenvironment modulation unmasks therapeutic benefit of radiotherapy and checkpoint inhibition. *J Immunother Cancer* 2019;7:216.

18 Philippou Y, Sjoberg HT, Murphy E, *et al*. Impacts of combining anti-PD-L1 immunotherapy and radiotherapy on the tumour immune microenvironment in a murine prostate cancer model. *Br J Cancer* 2020;123:1089–100.

19 Dudzinski SO, Cameron BD, Wang J, *et al*. Combination immunotherapy and radiotherapy causes an abscopal treatment response in a mouse model of castration resistant prostate cancer. *J Immunother Cancer* 2019;7:218.

20 Demaria S, Kawashima N, Yang AM, *et al*. Immune-mediated inhibition of metastases after treatment with local radiation and CTLA-4 blockade in a mouse model of breast cancer. *Clin Cancer Res* 2005;11:728–34.

21 Beer TM, Kwon ED, Drake CG, *et al*. Randomized, double-blind, phase III trial of ipilimumab versus placebo in asymptomatic or minimally symptomatic patients with metastatic Chemotherapy-Naive castration-resistant prostate cancer. *JCO* 2017;35:40–7.

22 Antonarakis ES, Piulats JM, Gross-Goupil M, *et al*. Pembrolizumab for treatment-refractory metastatic castration-resistant prostate cancer: Multicohort, open-label phase II KEYNOTE-199 study. *JCO* 2020;38:395–405.

23 Sweeney CJ, Gillessen S, Rathkopf D, *et al*. Abstract CT014: IMbassador250: a phase III trial comparing atezolizumab with enzalutamide vs enzalutamide alone in patients with metastatic castration-resistant prostate cancer (mCRPC). *Cancer Res* 2020;80:CT014.

24 Escorcia FE, Postow MA, Barker CA. Radiotherapy and immune checkpoint blockade for melanoma: a promising combinatorial strategy in need of further investigation. *Cancer J* 2017;23:32–9.

25 Demaria S, Bhardwaj N, McBride WH, *et al*. Combining radiotherapy and immunotherapy: a revived partnership. *Int J Radiat Oncol Biol Phys* 2005;63:655–66.

26 Lee Y, Auh SL, Wang Y, *et al*. Therapeutic effects of ablative radiation on local tumor require CD8+ T cells: changing strategies for cancer treatment. *Blood* 2009;114:589–95.

27 Theelen WSME, Peulen HMU, Lalezari F, *et al*. Effect of pembrolizumab after stereotactic body radiotherapy vs pembrolizumab alone on tumor response in patients with advanced non-small cell lung cancer: results of the PEMBRO-RT phase 2 randomized clinical trial. *JAMA Oncol* 2019;5:1276.

28 Kwon ED, Drake CG, Scher HI, *et al*. Ipilimumab versus placebo after radiotherapy in patients with metastatic castration-resistant prostate cancer that had progressed after docetaxel chemotherapy (CA184-043): a multicentre, randomised, double-blind, phase 3 trial. *Lancet Oncol* 2014;15:700–12.

29 Weichert JP, Clark PA, Kandela IK, *et al*. Alkylphosphocholine analogs for broad-spectrum cancer imaging and therapy. *Sci Transl Med* 2014;6:240ra75.

30 Grudzinski JJ, Titz B, Kozak K, *et al*. A phase 1 study of 131I-CLR1404 in patients with relapsed or refractory advanced solid tumors: dosimetry, biodistribution, pharmacokinetics, and safety. *PLoS One* 2014;9:e111652.

31 Ailawadhi S, Stiff PJ, Ibrahim E, *et al*. Fractionated dosing of CLR 131 in patients with relapsed or refractory multiple myeloma (RRMM). *Blood* 2019;134:144.

32 Longcor J, Oliver K, Friend J, *et al*. Interim evaluation of a targeted radiotherapeutic, CLR 131, in relapsed/refractory diffuse large B-cell lymphoma patients (R/R DLBCL). *Annals of Oncology* 2019;30:v435.

33 Longcor J, Phase OK. 1, open-label, dose escalation study of I-131-CLR1404 (CLR 131) in patients with relapsed or refractory multiple myeloma. *Blood* 1864;2019:134.

34 Grudzinski JJ, Hernandez R, Marsh I, *et al*. Preclinical characterization of 86/90Y-NM600 in a variety of murine and human cancer tumor models. *J Nucl Med* 2019:jnumed.118.224808.

35 Hernandez R, Grudzinski J, Aluicio-Sarduy E. 177Lu-NM600 TRT shows efficacy in a syngeneic murine model of breast cancer. *J Nucl Med* 2018;59:535.

36 Hernandez R, Walker KL, Grudzinski JJ, *et al*. 90Y-NM600 targeted radionuclide therapy induces immunologic memory in syngeneic models of T-cell Non-Hodgkin's Lymphoma. *Commun Biol* 2019;2:79.

37 et alPatel RB, Hernandez R, Carlson P. Low-dose targeted radionuclide therapy renders immunologically cold tumors responsive to immune checkpoint blockade. Science Translational Medicine [Internet], 2021. American Association for the Advancement of Science. Available: https://stm.sciencemag.org/content/13/602/eabb3631 [Accessed 20 Jul 2021].

38 Besemer AE, Yang YM, Grudzinski JJ, *et al*. Development and validation of rapid: a patient-specific Monte Carlo three-dimensional internal dosimetry platform. *Cancer Biother Radiopharm* 2018;33:155–65.

39 Bednarz B, Grudzinski J, Marsh I, *et al*. Murine-specific internal dosimetry for preclinical investigations of imaging and therapeutic agents. *Health Phys* 2018;114:450–9.

40 Marsh IR, Grudzinski J, Baiu DC, *et al*. Preclinical Pharmacokinetics and Dosimetry Studies of [124] I/ [131] I-CLR1404 for Treatment of Pediatric Solid Tumors in Murine Xenograft Models. *J Nucl Med* 2019;60:1414–20.

41 Johnson LE, Frye TP, Chinnasamy N, *et al*. Plasmid DNA vaccine encoding prostatic acid phosphatase is effective in eliciting autologous antigen-specific CD8+ T cells. *Cancer Immunol Immunother* 2007;56:885–95.

42 Dahan R, Sega E, Engelhardt J, *et al*. FcγRs modulate the anti-tumor activity of antibodies targeting the PD-1/PD-L1 axis. *Cancer Cell* 2015;28:285–95.

43 Kumagai S, Togashi Y, Kamada T, *et al*. The PD-1 expression balance between effector and regulatory T cells predicts the clinical efficacy of PD-1 blockade therapies. *Nat Immunol* 2020;21:1346–58.

44 Selby MJ, Engelhardt JJ, Quigley M, *et al*. Anti-CTLA-4 antibodies of IgG2a isotype enhance antitumor activity through reduction of intratumoral regulatory T cells. *Cancer Immunol Res* 2013;1:32–42.

45 Lahl K, Sparwasser T. In Vivo Depletion of FoxP3+ Tregs Using the DEREG Mouse Model. In: Kassiotis G, Liston A, eds. *Regulatory T Cells: Methods and Protocols [Internet]*. Totowa, NJ: Humana Press, 2011: 157–72. https://doi.org/10.1007/978-1-61737-979-6_10

46 Cao M, Cabrera R, Xu Y, *et al*. Gamma irradiation alters the phenotype and function of CD4+CD25+ regulatory T cells. *Cell Biol Int* 2009;33:565–71.

47 Qu Y, Jin S, Zhang A, *et al*. Gamma-ray resistance of regulatory CD4+CD25+Foxp3+ T cells in mice. *Radiat Res* 2010;173:148–57.

48 Balogh A, Persa E, Bogdándi EN, *et al*. The effect of ionizing radiation on the homeostasis and functional integrity of murine splenic regulatory T cells. *Inflamm. Res.* 2013;62:201–12.

49 Champiat S, Dercle L, Ammari S, *et al*. Hyperprogressive disease is a new pattern of progression in cancer patients treated by anti-PD-1/PD-L1. *Clinical Cancer Research* 2017;23:1920–8.

50 Kato S, Goodman A, Walavalkar V, *et al*. Hyperprogressors after immunotherapy: analysis of genomic alterations associated with accelerated growth rate. *Clinical Cancer Research* 2017;23:4242–50.

51 Wang X, Wang F, Zhong M, *et al*. The biomarkers of hyperprogressive disease in PD-1/PD-L1 blockage therapy. *Mol Cancer* 2020;19:81.

52 Kamada T, Togashi Y, Tay C, *et al*. PD-1 [+] regulatory T cells amplified by PD-1 blockade promote hyperprogression of cancer. *Proc Natl Acad Sci U S A* 2019;116:9999–10008.

53 Kang DH, Chung C, Sun P, *et al*. Circulating regulatory T cells predict efficacy and atypical responses in lung cancer patients treated with PD-1/PD-L1 inhibitors. *Cancer Immunol Immunother* 2022;71:579–88.